Satellite Attitude Control Using only Magnetorquers

Ping Wang, Yuri B. Shtessel and Yong-qian Wang
Department of Electrical & Computer Engineering
University of Alabama in Huntsville, Huntsville, AL. 35899
pwang@ebs330.eb.uah.edu

I. INTRODUCTION

Since magnetic control systems are relatively reliable, lightweight, and energy efficient, magnetic torque was found to be attractive for small, inexpensive satellites. Magnetorquers are often used with a gravity gradient boom to control a spacecraft's attitude[1][2]. However, the attempts at using only magnetorquers in all three axes have been unsuccessful, because control torque can only be generated perpendicular to the geomagnetic field vector.

This study presents a method to control small satellites only using magnetorquers. If the spacecraft is isoinertial, employing Krstic's backstepping concept[3], dynamics equation is divided into two parts in geomagnetic frame: the outer loop and the inner loop. The outer loop controller is regarded as a regulation system which is controlled by the virtual control input. Because the outer loop is a nonlinear and periodical system, and it's stability is supported by La Salle's and Floquet's theorems. The inner loop controller is designed for a tracking system and produces the signal to track the virtual control. Considering disturbance torque, a sliding mode controller is designed in the inner loop[4][5].

Simulation results show that three axis control can be achieved with magnetorquers as the sole actuators. The control system has a good performance not only in detumbling phase but also in attitude acquisition phase.

II. SPACECRAFT DYNAMICS AND KINEMATICS

1. Definition of Geomagnetic Frame

The coordinate systems used in spacecraft attitude dynamics usually are an earth center inertial frame (**Fi**), an orbit frame (**Fo**), and a body frame (**Fb**). Their definitions can be found in the reference[6]. Because the control torque generated by magnetorquers depends on the direction of the geomagnetic field, geomagnetic frame (**Fg**) is introduced in this study.

Definition: **Fg** is a coordinate system with the origin in the spacecraft center, and Xg axis is parallel to the geomagnetic field (**B**). Suppose the azimuth and elevation of **B** are α and β respectively in **Fo** (Fig. 1). **Fg** is attained by **Fo**'s principal rotations w.r.t. Zo and Yo axis, about α and β respectively.

$$\mathbf{F}_g = \mathbf{C}_{go}\mathbf{F}_o, \tag{1}$$

where $\mathbf{C}_{go}$ is the **Fg**'s rotation matrix w.r.t. **Fo**

$$\mathbf{C}_{go} = \begin{bmatrix} \cos\beta\cos\alpha & \cos\beta\sin\alpha & -\sin\beta \\ -\sin\alpha & \cos\alpha & 0 \\ \sin\beta\cos\alpha & \sin\beta\sin\alpha & \cos\beta \end{bmatrix}. \tag{2}$$

Obviously, magnetic field is $\mathbf{B} = \begin{bmatrix} b & 0 & 0 \end{bmatrix}^T$ in **Fg**, and $b = \|\mathbf{B}\|$ is the magnitude of **B**.

On the orbit, magnetic field **B** changes periodically, so α, β, and b are periodical functions. Suppose $\omega_{go} = \begin{bmatrix} a_1 & a_2 & a_3 \end{bmatrix}^T$ is the **Fg**'s angular velocity w.r.t. **Fo**, and it is also a periodical function. For a given orbit, α, β, b and ω_{go} can be calculated on the ground before hand.

2. Rotational Dynamics and Kinematics[6][7]

Provided **Fb** is chosen to be a principal-axis frame, the moment of inertial for the spacecraft is $\mathbf{J} = diag\{I_x \quad I_y \quad I_z\}$. Furthermore, if $I_x = I_y = I_z = \rho$ (the isoinertial case), the Earth pointing satellite's dynamics and kinematics model in **Fb** is

$$\dot{\mathbf{q}} = \frac{1}{2}\mathbf{T}(\mathbf{Q})\omega, \tag{3}$$

$$\dot{q}_4 = -\frac{1}{2}\omega^T\mathbf{q}, \tag{4}$$

$$\dot{\omega} + \dot{\mathbf{C}}_{bo}\omega_{oi} = \frac{1}{\rho}\mathbf{N}_c. \tag{5}$$

where $\mathbf{Q} = \begin{bmatrix} \mathbf{q}^T & q_4 \end{bmatrix}^T$ is the quaternions, and $\mathbf{q} = \begin{bmatrix} q_1 & q_2 & q_3 \end{bmatrix}^T$ is its vector part, which satisfies the restriction $\mathbf{q}^T\mathbf{q} + q_4^2 = 1$. The matrix $\mathbf{T}$ is defined as $\mathbf{T}(\mathbf{Q}) = q_4\mathbf{I}_{3\times3} + \mathbf{q}^\times$. $\omega_{oi} = \begin{bmatrix} 0 & -\omega_0 & 0 \end{bmatrix}^T$ is the orbital

0-7803-4547-9/98/$10.00 © 1998 IEEE

velocity. The orbital rate ω_0 can be regarded as a constant for small eccentricity orbit. $\mathbf{N}_c$ is the control torque. $\mathbf{C}_{bo}$ is the **Fb**'s rotation matrix w.r.t. **Fo**

$$\mathbf{C}_{bo} = \left(q_4^2 - \mathbf{q}^T\mathbf{q}\right)\mathbf{I}_{3\times 3} + 2\mathbf{q}\mathbf{q}^T - 2q_4\mathbf{q}^{\times}. \tag{6}$$

Note: To avoid the singularity in $\mathbf{T}^{-1}$ that occurs at $q_4 = 0$, the workspace is restricted as follows[6]:

$$\|\mathbf{q}\| \le \gamma < 1,\ q_4 \ge \sqrt{1-\gamma^2}.$$

III. DYNAMICS EQUATION IN GEOMAGNETIC FRAME

The magnetic control torque $\mathbf{N}_c = -\mathbf{B}^{\times}\mathbf{M}$ is always in the control plane which is perpendicular to the geomagnetic field vector **B** (Fig. 2). **M** is the magnetic dipole moment generated by magnetorquers. Since only the components of **M** which are in the control plane are effective, **M** can be expressed in **Fg** as

$$\mathbf{M} = \begin{bmatrix} 0 & m_2 & m_3 \end{bmatrix}^T. \tag{7}$$

$\mathbf{N}_c$ is described in **Fg** as

$$\mathbf{C}_{go}\mathbf{C}_{bo}^T\mathbf{N}_c = \begin{bmatrix} 0 & m_3 b & -m_2 b \end{bmatrix}^T \tag{8}$$

In order to employ backstepping concepts, it is necessary to express $\mathbf{q}$ and ω in **Fg**. Therefor let $\tilde{\omega} = \mathbf{C}_{go}\mathbf{C}_{bo}^T\omega$, $\tilde{\mathbf{q}} = \mathbf{C}_{go}\mathbf{C}_{bo}^T\mathbf{q}$, $u_1 = m_3 b/\rho$, and $u_2 = -m_2 b/\rho$. Considering that $\dot{\mathbf{C}}_{bo} = -\omega^{\times}\mathbf{C}_{bo}$, $\dot{\mathbf{C}}_{go} = -\omega_{go}^{\times}\mathbf{C}_{go}$, $\mathbf{C}_{bo}\mathbf{q} = \mathbf{q}$, and $\mathbf{T}(\mathbf{Q})\mathbf{C}_{bo} = q_4\mathbf{I}_{3\times 3} - \mathbf{q}^{\times}$. Eq. (3) and (5) can be transformed to:

$$\dot{\tilde{\mathbf{q}}} = -\omega_{go}^{\times}\tilde{\mathbf{q}} + \frac{1}{2}\left(q_4\mathbf{I}_{3\times 3} - \tilde{\mathbf{q}}^{\times}\right)\tilde{\omega} \tag{9}$$

$$\dot{\tilde{\omega}} = -\left(\omega_{go} + \mathbf{C}_{go}\omega_{oi}\right)^{\times}\tilde{\omega} + \begin{bmatrix} 0 & 0 \\ 1 & 0 \\ 0 & 1 \end{bmatrix}\begin{bmatrix} u_1 \\ u_2 \end{bmatrix}. \tag{10}$$

Eq. (9) and (10) can be rewritten as:

$$\begin{bmatrix} \dot{\tilde{q}}_1 \\ \dot{\tilde{q}}_2 \\ \dot{\tilde{q}}_3 \\ \dot{\tilde{\omega}}_1 \end{bmatrix} = \frac{1}{2}\begin{bmatrix} 0 & 2a_3 & -2a_2 & q_4 \\ -2a_3 & 0 & -2a_1 & -\tilde{q}_3 \\ 2a_2 & 2a_1 & 0 & \tilde{q}_2 \\ 0 & 0 & 0 & 0 \end{bmatrix}\begin{bmatrix} \tilde{q}_1 \\ \tilde{q}_2 \\ \tilde{q}_3 \\ \tilde{\omega}_1 \end{bmatrix} + \frac{1}{2}\begin{bmatrix} \tilde{q}_3 & -\tilde{q}_2 \\ q_4 & \tilde{q}_1 \\ -\tilde{q}_1 & q_4 \\ 2b_1 & 2b_2 \end{bmatrix}\begin{bmatrix} \tilde{\omega}_2 \\ \tilde{\omega}_3 \end{bmatrix} \tag{11}$$

$$\begin{bmatrix} \dot{\tilde{\omega}}_2 \\ \dot{\tilde{\omega}}_3 \end{bmatrix} = \begin{bmatrix} 0 & 0 & 0 & -b_1 \\ 0 & 0 & 0 & -b_2 \end{bmatrix}\begin{bmatrix} \tilde{q}_1 \\ \tilde{q}_2 \\ \tilde{q}_3 \\ \tilde{\omega}_1 \end{bmatrix} + \begin{bmatrix} 0 & c \\ -c & 0 \end{bmatrix}\begin{bmatrix} \tilde{\omega}_2 \\ \tilde{\omega}_3 \end{bmatrix} + \begin{bmatrix} 1 & 0 \\ 0 & 1 \end{bmatrix}\begin{bmatrix} u_1 \\ u_2 \end{bmatrix}, \tag{12}$$

where $b_1 = a_3 - \omega_0 \sin\alpha \sin\beta$, $b_2 = -a_2 + \omega_0 \cos\alpha$, and $c = a_1 - \omega_0 \cos\beta \sin\alpha$.

Remark: An apparent difficulty with this model is that the state $\begin{bmatrix} \tilde{q}_1 & \tilde{q}_2 & \tilde{q}_3 & \tilde{\omega}_1 \end{bmatrix}^T$ is only indirectly related to the input u_1, u_2, through the state variable $\begin{bmatrix} \tilde{\omega}_2 & \tilde{\omega}_3 \end{bmatrix}^T$ and nonlinear state equation (11). Therefore, it is not easy to see how the input u_1, u_2 can be designed to control $\begin{bmatrix} \tilde{q}_1 & \tilde{q}_2 & \tilde{q}_3 & \tilde{\omega}_1 \end{bmatrix}^T$. However, the difficulty of control design can be reduced by the backstepping concept if we regard $\begin{bmatrix} \tilde{\omega}_2 & \tilde{\omega}_3 \end{bmatrix}^T$ as virtual control of Eq. (11). The controller's structure is composed of two parts: the outer loop and inner loop, which will be introduced in the order.

IV. OUTER LOOP CONTROLLER DESIGN

In the outer loop, $\begin{bmatrix} \tilde{\omega}_2 & \tilde{\omega}_3 \end{bmatrix}^T$ is considered as a virtual control for $\begin{bmatrix} \tilde{q}_1 & \tilde{q}_2 & \tilde{q}_3 & \tilde{\omega}_1 \end{bmatrix}^T$ described by Eq.(11). The goal is to find the control law

$$\omega_i^* = \tilde{\omega}_i\left(\tilde{q}_1 \quad \tilde{q}_2 \quad \tilde{q}_3 \quad \tilde{\omega}_1\right)^T,\ i = 2,\ 3 \tag{13}$$

such that $\tilde{q}_1$, $\tilde{q}_2$, $\tilde{q}_3$, $\tilde{\omega}_1$ tend to zero. Substituting ω_i^* for $\tilde{\omega}_i$, the outer loop dynamics is rewritten as

$$\begin{bmatrix} \dot{\tilde{q}}_1 \\ \dot{\tilde{q}}_2 \\ \dot{\tilde{q}}_3 \\ \dot{\tilde{\omega}}_1 \end{bmatrix} = \frac{1}{2}\begin{bmatrix} 0 & 2a_3 & -2a_2 & q_4 \\ -2a_3 & 0 & -2a_1 & -\tilde{q}_3 \\ 2a_2 & 2a_1 & 0 & \tilde{q}_2 \\ 0 & 0 & 0 & 0 \end{bmatrix}\begin{bmatrix} \tilde{q}_1 \\ \tilde{q}_2 \\ \tilde{q}_3 \\ \tilde{\omega}_1 \end{bmatrix} + \frac{1}{2}\begin{bmatrix} \tilde{q}_3 & -\tilde{q}_2 \\ q_4 & \tilde{q}_1 \\ -\tilde{q}_1 & q_4 \\ 2b_1 & 2b_2 \end{bmatrix}\begin{bmatrix} \omega_1^* \\ \omega_2^* \end{bmatrix} \tag{14}$$

The satellite's attitude control progress is usually divided into two phases: detumbling and attitude acquisition. The control laws in these two phases are discussed below.

1. Control law 1 -- Detumbling control

After it is released from the launch vehicle, the satellite is tumbling randomly with known bounds on the initial angular rate. The objective of this phase is to reduce angular velocity. The control law is:

$$\begin{bmatrix} \omega_2^* \\ \omega_3^* \end{bmatrix} = -k^d\begin{bmatrix} b_1 \\ b_2 \end{bmatrix}\tilde{\omega}_1, \tag{15}$$

where $k^d > 0$.

Apparently, from Eq. (14), $\dot{\tilde{\omega}}_1 = -k^a\left(b_1^2 + b_2^2\right)\tilde{\omega}_1$, and $\tilde{\omega}$ tends to zero while time tends to infinity.

2. Control law2 -- Attitude Acquisition

After the phase of detumbling, we will adjust attitude letting **q** approach zero while ω is zero. The control law is designed as follows:

$$\omega_2^* = -k_1^a\left[\tilde{q}_2 + 2b_1k_2^a\left(\tilde{\omega}_1 + k_3^a\tilde{q}_1\right)\right]$$
$$\omega_3^* = -k_1^a\left[\tilde{q}_3 + 2b_2k_2^a\left(\tilde{\omega}_1 + k_3^a\tilde{q}_1\right)\right], \qquad (16)$$

where $k_i^a > 0$, $i = 1, 2, 3$.

Now a simple explanation about the control law (16) is in order. Since $|a_i|$ and $|b_i|$ are much less than 1, if the bias of $\tilde{q}_1$, $\tilde{q}_2$, $\tilde{q}_3$ is large, the items of a_i and b_j in Eq. (14) and (16) can be omitted. As a result, we have

$$\dot{\tilde{q}}_1 = \frac{1}{2}\left(q_4\tilde{\omega}_1 + \tilde{q}_3\omega_2^* - \tilde{q}_2\omega_3^*\right)$$
$$\dot{\tilde{q}}_2 = \frac{1}{2}\left(-\tilde{q}_3\tilde{\omega}_1 + q_4\omega_2^* + \tilde{q}_1\omega_3^*\right)$$
$$\dot{\tilde{q}}_3 = \frac{1}{2}\left(\tilde{q}_2\tilde{\omega}_1 - \tilde{q}_1\omega_2^* + q_4\omega_3^*\right) \qquad (17)$$
$$\omega_2^* = -k_1^a\tilde{q}_2$$
$$\omega_3^* = -k_1^a\tilde{q}_3 \qquad (18)$$

To analyze the asymptotic stability of the system (17) and (18), the following candidate to a Lyapunov function is introduced by the way of the equation

$$V = \tilde{q}_1^2 + \tilde{q}_2^2 + \tilde{q}_3^2 > 0. \qquad (19)$$

From Eq. (17) and (18),

$$\dot{V} = -k_1^a q_4\left(\tilde{q}_2^2 + \tilde{q}_3^2\right) + \tilde{q}_1 q_4\tilde{\omega}_1, \qquad (20)$$

Assuming that $\tilde{\omega}_1$ keeps within a very small domain after detumbling, the item of $\tilde{q}_1 q_4\tilde{\omega}_1$ can be omitted. $\dot{V}$ is negative semi-definite. According to La Salle's invariant set theorems[8], the invariant set is $\tilde{q}_2 = 0$ and $\tilde{q}_3 = 0$. The motion on this set is described by the following equations:

$$\dot{\tilde{q}}_1 = \frac{1}{2}q_4\tilde{\omega}_1 \qquad (21)$$
$$\dot{\tilde{\omega}}_1 = -2k_1^a k_2^a\left(b_1^2 + b_2^2\right)\left(\tilde{\omega}_1 + k_3^a\tilde{q}_1\right). \qquad (22)$$

Note: When calculating $\tilde{\omega}_1$, we cannot omit b_j, otherwise $\tilde{\omega}_1$ is uncontrollable.

Let $\tilde{q}_1 = \sin\lambda$, then $q_4 = \cos\lambda$, because $q_4 = \sqrt{1-\tilde{q}_1^2}$ when $\tilde{q}_2 = 0$, $\tilde{q}_3 = 0$. From Eq. (21) and (22), we derive the following:

$$\dot{\lambda} = \frac{1}{2}\tilde{\omega}_1 \qquad (23)$$
$$\dot{\tilde{\omega}}_1 = -2k_1^a k_2^a\left(b_1^2 + b_2^2\right)\left(\tilde{\omega}_1 + k_3^a\sin\lambda\right) \qquad (24)$$

Obviously, λ does approach zero.

The analysis above shows that $\tilde{q}_1$, $\tilde{q}_2$, $\tilde{q}_3$ will approach to zero when their errors are large. When $\tilde{q}_1$, $\tilde{q}_2$, $\tilde{q}_3$ enter into a small vicinity of origin, we can linearize the Eq. (14) and (16) at the neighborhood of origin

$$\dot{\mathbf{x}}_1(t) = \mathbf{A}_1(t)\mathbf{x}_1(t) + \mathbf{B}_1(t)\mathbf{u}_1(t) \qquad (25)$$
$$\mathbf{u}_1(t) = \mathbf{K}_1(t)\mathbf{x}_1(t) \qquad (26)$$

where

$$\mathbf{x}_1 = \left[\tilde{q}_1 \quad \tilde{q}_2 \quad \tilde{q}_3 \quad \tilde{\omega}_1\right]^T,\ \mathbf{u}_1(t) = \left[\omega_1^* \quad \omega_2^*\right]^T$$

$$\mathbf{A}_1(t) = \begin{bmatrix} 0 & a_3 & -a_2 & 0.5 \\ -a_3 & 0 & -a_1 & 0 \\ a_2 & a_1 & 0 & 0 \\ 0 & 0 & 0 & 0 \end{bmatrix},\ \mathbf{B}_1(t) = \begin{bmatrix} 0 & 0 \\ 0.5 & 0 \\ 0 & 0.5 \\ b_1 & b_2 \end{bmatrix}$$

$$\mathbf{K}_1(t) = \begin{bmatrix} -2k_1^a k_2^a k_3^a b_1 & -k_1^a & 0 & -2k_1^a k_2^a b_1 \\ -2k_1^a k_2^a k_3^a b_2 & 0 & -k_1^a & -2k_1^a k_2^a b_2 \end{bmatrix}.$$

Because

$\mathbf{A}_1(t+T) = \mathbf{A}_1(t)$, $\mathbf{B}_1(t+T) = \mathbf{B}_1(t)$, $\mathbf{K}_1(t+T) = \mathbf{K}_1(t)$, obviously, the close loop is a linear periodical system.

According to Floquet's theorems[8], if for the close loop system

$$\mathbf{A}_c(t) = \mathbf{A}_1(t) + \mathbf{B}_1(t)\mathbf{K}_1(t), \qquad (27)$$

the characteristic multipliers belong to the open unit circle, then the close loop is asymptotically stable. So the local stability of the close loop can be judged by Floquet's theorems.

V. INNER LOOP CONTROLLER DESIGN

The inner loop is to control $\left[\tilde{\omega}_2 \quad \tilde{\omega}_3\right]^T$ which tracks the virtual control signal $\left[\omega_2^* \quad \omega_3^*\right]^T$ in terms of Eq. (12). Considering the disturbance torque, a sliding mode controller is used. The dynamics equation of the inner loop is rewritten as follows,

$$\dot{\mathbf{x}}_2 = \mathbf{A}_2(t)\mathbf{x}_2 + \mathbf{f} + \mathbf{u}_2 + \mathbf{d} \qquad (28)$$

where

$$\mathbf{x}_2 = \left[\tilde{\omega}_1 \quad \tilde{\omega}_2\right]^T,\ \mathbf{f} = \left[-b_1\tilde{\omega}_1 \quad -b_2\tilde{\omega}_1\right],\ \mathbf{u}_2 = \left[u_1 \quad u_2\right]^T,$$

and $\mathbf{A}_2(t) = \begin{bmatrix} 0 & c \\ -c & 0 \end{bmatrix}$,

$\mathbf{d} = \left[d_1 \quad d_2\right]^T$ is the component of disturbance torque in the control plane.

Let $\mathbf{x}_d = \left[\omega_1^* \quad \omega_2^*\right]^T$. The desired sliding surface is

$$\mathbf{S} = \mathbf{x}_d - \mathbf{x}_2 = 0. \qquad (29)$$

In order to provide asymptotic stability of $\mathbf{S}=0$, the following candidate Lyapunov function is selected:

$$V=\frac{1}{2}\mathbf{S}^T\mathbf{S}. \tag{30}$$

The derivative of V is identified

$$\dot{V}=\mathbf{S}^T\left[\dot{\mathbf{x}}_d-\mathbf{A}_2(t)\mathbf{x}_2-\mathbf{f}-\mathbf{u}_2-\mathbf{d}\right] \tag{31}$$

Selecting the control torque in the following format:

$$\mathbf{u}_2=\mathbf{u}_{eq}+R\mathbf{sign}(\mathbf{S}) \tag{32}$$

where:

$$\mathbf{u}_{eq}=-\dot{\mathbf{x}}_d+\mathbf{A}_2(t)\mathbf{x}_2+\mathbf{f}, \tag{33}$$

and $R>\max\|\mathbf{d}\|$. It is found that

$$\dot{V}=-R\sum_{i=1}^{2}|s_i|-\sum_{i=1}^{2}s_i\cdot d_i<0, \tag{34}$$

which guarantees the state will converge to a sliding surface under the control law (32).

In order to erase chattering, the sign function is replaced with the saturation function. The saturation function is defined as:

$$sat\left(\frac{s_i}{\varepsilon}\right)=\begin{cases}1 & s_i>\varepsilon\\ \dfrac{s_i}{\varepsilon} & |s_i|\le\varepsilon\\ -1 & s_i<-\varepsilon\end{cases}, \tag{35}$$

where ε is the thickness of the sliding boundary layer.

VI. NUMERICAL EXAMPLES

The validity of this method can be demonstrated by the following example. The moments of inertia about a spacecraft are assumed to be $Ix=Iy=Iz=10$ Kg-m^2. The spacecraft is assumed to be in circular pole orbit at the altitude of 675 Km, where $\omega_0=0.00107$ rad/s. At the pole orbit, the magnetic field in **Fb** can be simply expressed as [7]

$$\begin{aligned}x_o&=-\frac{\mu_m}{r^3}\cos\omega_0(t-t_0)\\ y_o&=0\\ z_o&=-\frac{2\mu_m}{r^3}\sin\omega_0(t-t_0)\end{aligned} \tag{36}$$

where r represents distance from the geocenter and $\mu_m=1\times10^{17}$ Wb-m is Earth's dipole strength. In this case, $a_1(t)=a_3(t)=0$, $b_1(t)=0$. $a_2(t)$ and $b_2(t)$ are shown in Fig. 3 and 4.

The detumbling controller is designed as follows:

$k^d=1000.$; $R=0.01$; $\varepsilon=0.01$.

Fig. 5 shows typical ω trajectories.

On the attitude acquisition phase, the controller is designed as

$k_1^a=0.002$; $k_2^a=2000$; $k_3^a=0.4$; $R=0.01$; $\varepsilon=0.01$.

If we linearize the Eq. (14) and (16), the characteristic multipliers of the close loop system (27) are

$0.32+0.64i$, $0.32-0.64i$, 0.72, and 0.37.

Because all of them are in the open unit circle, the original system is local stable. The simulation of attitude acquisition is shown in fig. 6 and 7.

VII. CONCLUSION

This study has addressed a practical attitude control method for a small satellite with magnetorquer control only. The outer loop and inner loop controller are designed according to the backstepping concept. Different control laws are designed for the phases of detumbling and attitude acquisition respectively. The results of the stability analysis and simulation show that three axis control can be attained with magnetorquers as the sole actuators in low Earth orbit.

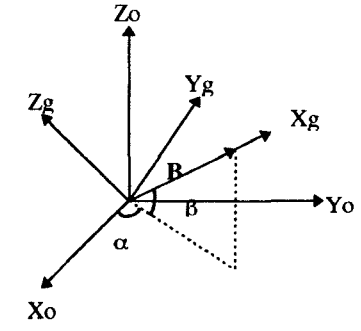

Fig.1 The relation between **Fg** and **Fo**

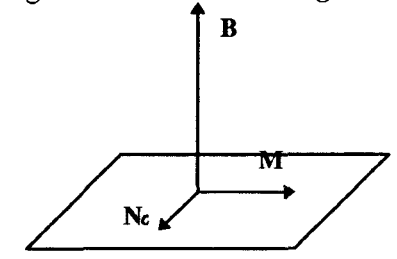

Control Plane

Fig. 2 The control plane

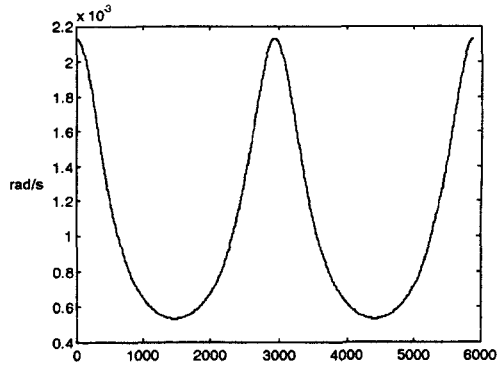

Time (Sec)

Fig.3 The variety of $a_2(t)$ in the orbit

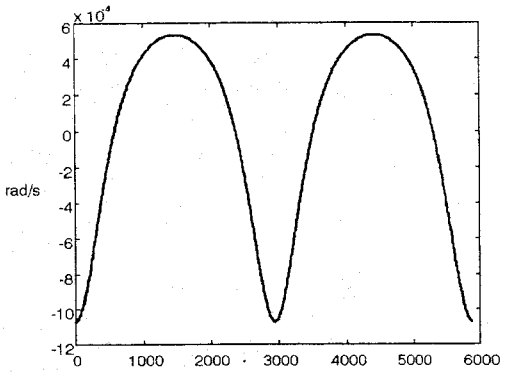

Time (Sec)

Fig.4 The variety of $b_2(t)$ in the orbit

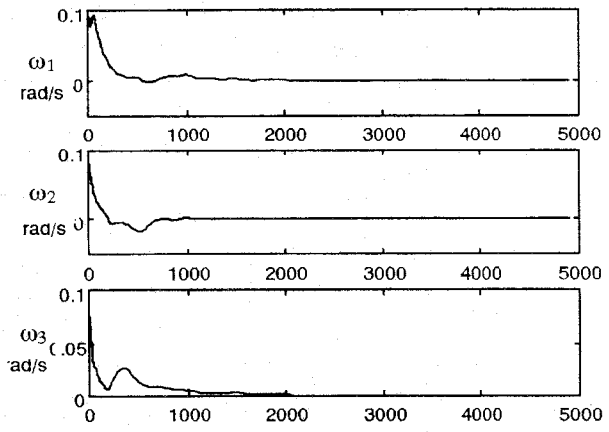

Time (Sec)

Initial condition: $q = \begin{bmatrix} 0.9 & 0 & 0 \end{bmatrix}^T$,

$\omega = \begin{bmatrix} 0.09 & 0.09 & 0.09 \end{bmatrix}^T$.

Fig.5 Angular velocity history in detumbling phase.

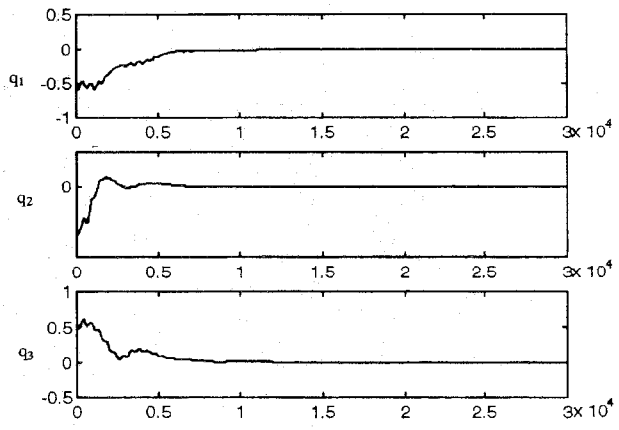

Time (Sec)

Initial condition: Same to Fig. (7).

Fig. 6. Attitude history in attitude acquisition

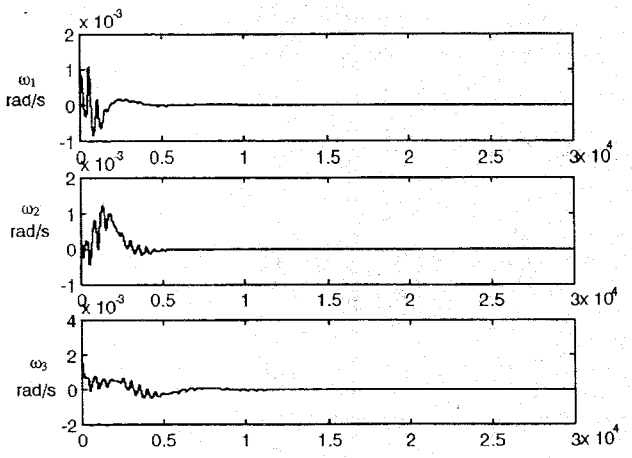

Time (Sec)

Initial condition: $q = \begin{bmatrix} -0.5 & -0.3 & 0.5 \end{bmatrix}^T$,

$\omega = \begin{bmatrix} -0.0001 & -0.0002 & 0.001 \end{bmatrix}^T$

Fig.7 Angular velocity history in attitude acquisition.

References

[1] Francois Martel, et.al., "Active Magnetic Control System for Gravity Gradient Stabilized Spacecraft," _____.

[2] Wishiewski, R., "Optimal Three-Axis Satellite Attitude Control with Use of Magnetic Torquing," AIAA Guidance, Navigation, and Control Conference, New Orleans, 1997.

[3] Krstic, Miroslav., Nonlinear and Adaptive Control Design, John, Wiley & Sons, Inc. 1991

[4] Utkin, V. I., Sliding Modes in Control Optimization Springer Verlag, NY, 1992.

[5] Decarlo, R. A., Zak, S.H., and Mathews, G.P., "Variable Structure Control of Nonlinear Multivariable Systems: A Tutorial," Proc. IEEE, vol. 76, no. 3, 1988

[6] Wertz, J. R., Spacecraft Attitude Determination and Control, Reidel, Dordrecht, The Netherlands, 1980.

[7] Hughs, Peter C., Spacecraft Attitude Dynamics, John, Wiley & Sons, Inc. 1986

[8] Slotine, J.J.E. and Li, W., Applied Nonlinear Control, Prentice-Hall, Englewood Cliffs, N.J., 1991

[9] Mohler. R.R. Nonlinear Systems Vol. Dynamics and Contro,. Prentice Hall. 1995